

# Similarities Between Polyelectrolyte Gels and Biopolymer Solutions

FERENC HORKAY,<sup>1</sup> ANNE-MARIE HECHT,<sup>2</sup> ERIK GEISLER<sup>2</sup>

<sup>1</sup>Section on Tissue Biophysics and Biomimetics, Laboratory of Integrative and Medical Biophysics, NICHD, National Institutes of Health, Bethesda, Maryland 20892

<sup>2</sup>Laboratoire de Spectrométrie Physique, CNRS UMR 5588, Université J. Fourier de Grenoble, B.P.87, 38402 St Martin d'Hères cedex, France

Received 30 May 2006; revised 26 July 2006; accepted 17 August 2006

DOI: 10.1002/polb.21008

Published online in Wiley InterScience (www.interscience.wiley.com).

**ABSTRACT:** Small angle neutron scattering (SANS) measurements and osmotic swelling pressure measurements are reported for polyelectrolyte gels and solutions under nearly physiological conditions. A synthetic polymer (sodium-polyacrylate) and three biopolymers (DNA, hyaluronic acid, and polyaspartic acid) are studied. The neutron scattering response of these anionic polyelectrolytes is closely similar, indicating that at larger length scales the organization of the polymer molecules is not significantly affected by the fine details of the molecular architecture (*e.g.*, size and chemical structure of the monomer unit, type of polymer backbone). The results suggest that specific interactions between the polyelectrolyte chains and the surrounding monovalent cations are negligible. It is found that the osmotic compression modulus of these biopolymer solutions determined from the analysis of the SANS response decreases with increasing chain persistence length. ©2006 Wiley Periodicals, Inc. *J Polym Sci Part B: Polym Phys* 44: 3679–3686, 2006

**Keywords:** biopolymers; gels; neutron scattering; osmotic modulus; swelling pressure

## INTRODUCTION

Charged polymers are important in many fields, in industry and in fundamental science ranging from physics to biology. Many important biological macromolecules are polyelectrolytes. Virtually all properties of polyelectrolyte solutions are governed by the electrostatic interactions. Katchalsky et al.<sup>1</sup> and Katchalsky and Michaeli<sup>2</sup> observed that collapse and expansion of charged polymer molecules occurred reversibly by adjusting the pH of the system. Tanaka and coworkers<sup>3–5</sup> discovered that in response to small changes in external conditions, such as temperature, electric field, or solvent and ionic composition, a gel can swell to many times its

original size or collapse into densely packed structures. They developed theoretical models to describe the swelling kinetics,<sup>4</sup> volume phase transitions, and critical phenomena of gels.<sup>3</sup>

In biopolymer systems such as polynucleic acids, proteins, biological membranes, in which macromolecules are dissolved in water containing different ions, electrostatic interactions often play a central role in determining the phase behavior.<sup>6,7</sup> Accurate theoretical description of electrostatic forces is however difficult. Polyelectrolytes dissociate in solution forming a strongly negatively charged polyanion surrounded by an atmosphere of small mobile counterions. Understanding the interaction of polyelectrolytes with ions could help to clarify the basic physics of ion binding as well as the mechanism of various biological processes. In certain biological systems, ion-polymer interactions lead to changes in the shape and size of the

Correspondence to: F. Horkay (E-mail: horkay@helix.nih.gov)

*Journal of Polymer Science: Part B: Polymer Physics*, Vol. 44, 3679–3686 (2006)  
©2006 Wiley Periodicals, Inc.

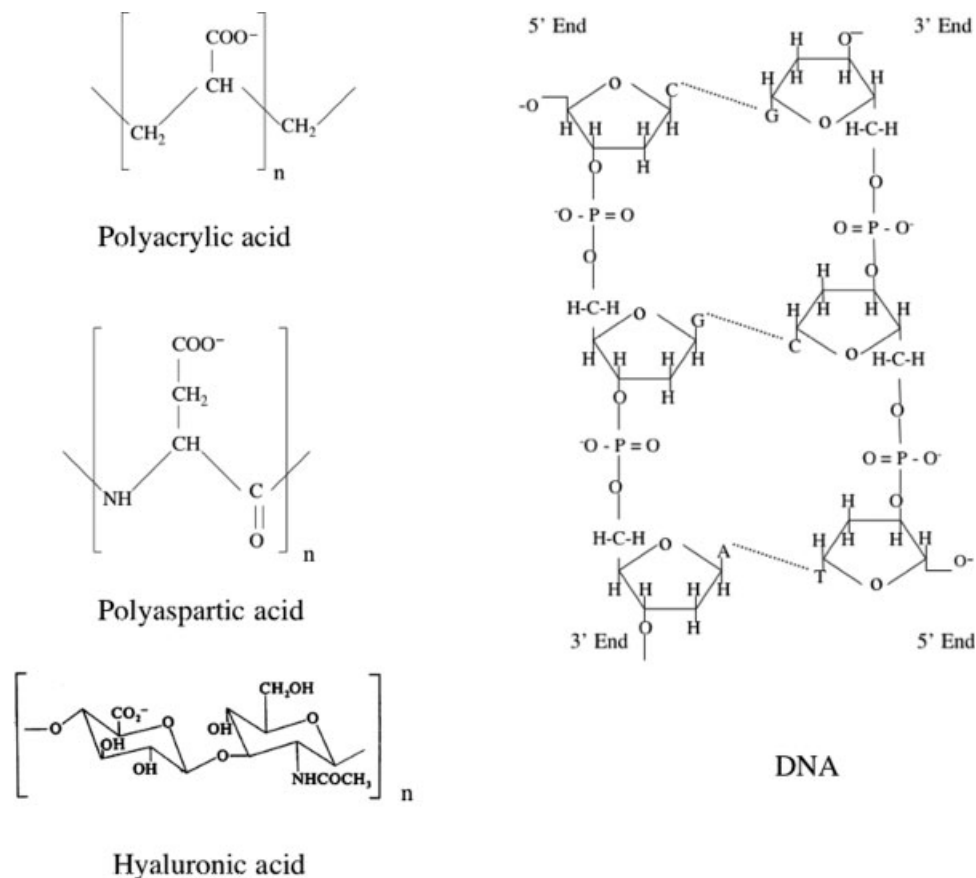


**Figure 1.** Chemical structure of the polyelectrolyte molecules investigated in the present work.

constituent chains. For example, DNA molecules in aqueous solution in the presence of high valence cations (*e.g.*, spermidine) form toroidal condensates.<sup>8,9</sup> In the course of the condensation process the highly swollen dilute system, in which the individual chains are separate, collapses into a densely packed arrangement of overlapping coils. Structure formation is the result of a complex interplay between thermodynamic and kinetic factors that depends on the interactions between the ions and the polymer molecules. Consequently, our ability to predict and describe polyelectrolyte behavior is a key element for understanding the properties of biopolymer systems.

The aim of the present work is to gain insight into the effect of ion-polymer interactions on the organization of dissolved macromolecules using small angle neutron scattering (SANS) together with macroscopic osmotic pressure measurements. Previous studies suggest that synthetic polyelectrolyte gels may “mimic” the physical-chemical properties of biopolymer gels, and the results

obtained for synthetic polymers can be extrapolated to biological systems.<sup>6,7,10</sup> This paper describes and compares some of the properties in both types of network. The results are analyzed according to the present status of the physics of gels. We report osmotic and scattering measurements for a synthetic polymer (polyacrylic acid sodium salt, PAA) and three biopolymers: DNA, hyaluronic acid (HA), and polyaspartic acid (PASP). Figure 1 shows the building blocks of the polymer chains. Although it is known that the chemical and physical properties of these polymers are significantly different, it is unclear how these differences affect their organization and thermodynamic behavior in nearly physiological salt solutions. We address the following specific questions: Do synthetic and biological polyelectrolytes exhibit similar structural and osmotic properties? How does the type of the chemical backbone affect the scattering response of biopolymer solutions? What is the effect of chemical crosslinks on the scattering and osmotic properties?

These questions have not yet been investigated in biopolymer systems.

## THEORY

### SANS from Polymer Solutions

In solutions of overlapping flexible polymer coils, the scattering intensity can be described by<sup>11,12</sup>

$$I_{\text{os}}(q) = \Delta\rho^2 \frac{k_B T \varphi^2}{K_{\text{os}}} \frac{1}{(1 + q^2 \xi^2)} \quad (1)$$

where  $\Delta\rho^2$  is the contrast factor between polymer and solvent,  $\varphi$  is the volume fraction of the polymer,  $q = \frac{4\pi}{\lambda} \sin \frac{\theta}{2}$  is the transfer wavevector,  $\lambda$  the wavelength of the incident radiation,  $\theta$  the angle of observation,  $\xi$  is the polymer-polymer correlation length in the solution,  $k_B$  the Boltzmann constant,  $T$  the absolute temperature, and  $K_{\text{os}}$  is the osmotic modulus.

If the polymer consists of rod-like molecules, then, by analogy with eq 1, the scattering intensity of semidilute polymer solutions can be expressed as<sup>13</sup>

$$I_{\text{os}}(q) = \Delta\rho^2 \frac{k_B T \varphi^2}{K_{\text{os}}} \frac{1}{(1 + qL)(1 + q^2 r_c^2)} \quad (2)$$

where  $L$  is the length of the rod and  $r_c$  its radius of cross section.

### Scattering from Inhomogeneous Polymer Gels

Introducing crosslinks into a neutral polymer solution favors the formation of large-scale clusters. As the gelation reaction proceeds these regions are subsequently frozen-in by the permanent crosslinks. Network inhomogeneities can be thought of as densely crosslinked clusters embedded in a weakly crosslinked ("solution-like") matrix. The total scattering intensity from polymer gels can usually be described as a sum of thermodynamic and frozen-in components<sup>14–16</sup>

$$I(q) = I_{\text{os}}(q) + I_{\text{clus}}(q) \quad (3)$$

where  $I_{\text{os}}(q)$  is governed by the osmotically driven concentration fluctuations and the second term,  $I_{\text{clus}}(q)$ , depends on the size and internal structure of the clusters. If the clusters are very large, scattering from their surfaces may dominate.<sup>17,18</sup> In many cases surface scattering can be described by a power law of the form

$$I_{\text{clus}}(q) = Aq^{-m} \quad (4)$$

where  $A$  is a constant and the exponent  $m$  is defined by  $3 < m \leq 4$  for surface scattering. Com-

binning eqs 2–4 yields<sup>16</sup>

$$I(q) = \Delta\rho^2 \frac{k_B T \varphi^2}{K_{\text{os}}} \frac{1}{(1 + qL)(1 + q^2 r_c^2)} + Aq^{-m} \quad (5)$$

Equation 5 provides a means to discriminate the osmotically driven concentration fluctuations from the total scattering intensity.

## EXPERIMENTAL

### Gel Preparation

Sodium polyacrylate (PAA) gels were prepared by free-radical copolymerization of acrylic acid and  $N,N'$ -methylenebis(acrylamide) crosslinker in aqueous solution according to a procedure described previously.<sup>19</sup> The monomer concentration was 30% (w/w), and 35% of the acrylic acid monomers were neutralized by sodium hydroxide prior to polymerization. Oxygen was removed by bubbling nitrogen through the solution. Ammonium persulfate (0.5 g/L) was used as initiator. The crosslinking process was carried out at 80 °C. After gelation gel samples were completely neutralized, and washed with deionized water to remove all extractable materials (e.g., unreacted crosslinker, sol fraction). Water was renewed every day for two weeks.

DNA gels were made from deoxyribonucleic acid sodium salt (prepared from salmon testes, Sigma).<sup>20</sup> The % G-C content of this DNA was 41.2%. The molecular weight determined by ultracentrifugation was  $1.3 \times 10^6$  Da, which corresponds to approximately 2000 base pairs. DNA was dissolved in HEPES buffer (pH = 7.0) and the solutions were dialyzed against distilled water. DNA gels were made by crosslinking<sup>20</sup> with ethyleneglycol diglycidyl ether in solution [pH = 9.0,  $c_{\text{DNA}} = 3\%$  (w/w)]. TEMED was used to adjust the pH.

PAA and DNA gels were equilibrated with NaCl solutions containing different amounts of  $\text{CaCl}_2$ . In both gel systems, at higher  $\text{CaCl}_2$  concentration phase separation occurs.<sup>19–21</sup> SANS and osmotic swelling pressure measurements were performed below this threshold concentration.

HA gels were made from HA solutions using a procedure similar to that described for the DNA gels. HA solutions were prepared from the sodium salt of HA (Sigma  $M_w = 1.2 \times 10^6$  Da) in 100 mM NaCl. Ethyleneglycol diglycidyl ether was used as crosslinker. Crosslinking was carried out at pH = 9 in the presence of TEMED.

After gelation both DNA and HA gels were washed to remove impurities (*e.g.*, unreacted cross-linker, TEMED) and then equilibrated with 100 mM NaCl solutions.

The pH (= 7) was identical in all samples.

### Preparation of Biopolymer Solutions

DNA solutions were made from the same DNA as the gels described earlier. The DNA concentration was 3% (w/w).

Sodium hyaluronate (HA, Sigma  $M_w = 1.2 \times 10^6$  Da) was dissolved at room temperature in 100 mM NaCl at pH = 7. The HA concentration of the solution was 3% (w/w).

PASP solution was prepared from PASP sodium salt (Sigma–Aldrich) in 100 mM NaCl at pH = 7. The low molecular weight polymer fraction was removed by dialysis. The molecular weight of the dialyzed PASP sample was 42 kDa.

### Small Angle Neutron Scattering Measurements

SANS measurements were carried out on the NG3 instrument at NIST, Gaithersburg, MD, using an incident wavelength  $\lambda = 8 \text{ \AA}$ . Solution and gel samples were placed in scattering cells with quartz windows and 2 mm path length, the temperature during the experiments being maintained at  $25 \pm 0.1 \text{ }^\circ\text{C}$ . The transfer wavevector explored in the experiments covered the range  $2.8 \times 10^{-3} \text{ \AA}^{-1} < q < 0.2 \text{ \AA}^{-1}$ . After azimuthal averaging, corrections for incoherent background, detector response, and cell window scattering were applied.<sup>22</sup>

### Osmotic Measurements

Osmotic swelling pressure measurements were made on gels using a method described elsewhere.<sup>23</sup> Gels were equilibrated with aqueous solutions of poly(vinyl pyrrolidone) (PVP, molecular weight: 29 kDa) of known osmotic pressure.<sup>24</sup> The gels were separated from the polymer solution by a semipermeable membrane (dialysis bag) to prevent penetration of the PVP molecules into the swollen network. At equilibrium, the swelling pressure of the gel is equal to the osmotic pressure of the PVP solution outside. The reversibility of the swelling/shrinking process was checked by reswelling the deswollen gels in solutions of known water activity.

### Elastic Modulus Measurements

Uniaxial compression measurements were made on gel cylinders in equilibrium with salt solutions

using a TA.XT2I HR Texture Analyser (Stable Micro Systems, UK). This apparatus measures the uniaxial deformation ( $\pm 0.001 \text{ mm}$ ) as a function of the applied force ( $\pm 0.01 \text{ N}$ ). Measurements were performed at deformation ratios  $0.7 < \Lambda < 1$ . The absence of volume change and barrel distortion during these measurements was checked. The elastic (shear) modulus,  $G$ , was calculated from the nominal stress,  $\sigma$  (force per unit undeformed cross section), using the equation<sup>19,25</sup>

$$\sigma = G(\Lambda - \Lambda^{-2}) \quad (6)$$

All measurements were made at  $25 \pm 0.1 \text{ }^\circ\text{C}$ .

## RESULTS AND DISCUSSION

Under physiological conditions, neutralized polyelectrolyte molecules dissociate in solution. The type and valence of the cations strongly influence the equilibrium properties of the charged polymer. Drastic changes in chain configuration can be induced by small changes in external conditions (*e.g.*, ionic strength and composition, pH).<sup>1–7,19</sup> In response to changes in the ionic composition, the conformation of the polymer molecules is modified and the gel swells or shrinks. Monovalent and multivalent ions act differently.<sup>21</sup>

The variation of the swelling degree with the  $\text{CaCl}_2$  concentration is shown in Figure 2(a) for weakly crosslinked PAA and DNA gels swollen in 40 mM NaCl solutions. At higher  $\text{CaCl}_2$  concentrations, both gels collapse, that is they expel a large amount of solvent and shrink. The diagram reveals three distinct regions: the first is below the “critical  $\text{CaCl}_2$  concentration”, in which the increase in ion concentration causes a monotonic decrease in swelling degree; the second region is in the vicinity of the critical concentration; and the third is above the critical concentration. Close to the transition, very small changes in ion composition cause dramatic changes in gel swelling. In the second region the shape of the swelling curve resembles the “cooperative” response observed in certain biological systems (*e.g.*, nerve excitation). In the third region any further increase in calcium concentration produces only a moderate volume change.

The dependence of the osmotic swelling pressure of PAA and DNA gels as a function of the polymer volume fraction is illustrated in Figure 2(b). The measurements were made in 40 mM NaCl solutions at constant  $\text{CaCl}_2$  concentrations. As the

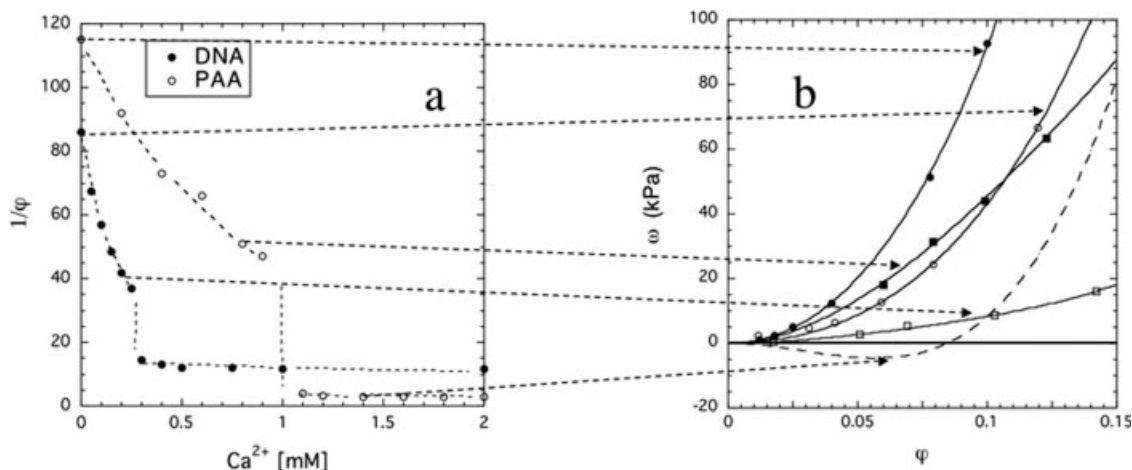


**Figure 2.** Variation of the swelling degree,  $1/\phi$ , of PAA ( $\circ$ ) and DNA ( $\bullet$ ) gels as a function of  $\text{CaCl}_2$  concentration in the surrounding 40 mM NaCl solution (a). Dependence of the swelling pressure of PAA and DNA gels on the polymer volume fraction at constant  $\text{CaCl}_2$  concentrations (b). Continuous curves show the fits to eq 7.

$\text{CaCl}_2$  concentration increases, the swelling pressure decreases. The continuous curves through the data points show the least squares fit to a Flory-Huggins type equation<sup>26</sup>

$$\omega = -(RT/v_1)[\ln(1-\phi) + \phi + \chi_0\phi^2 + \chi_1\phi^3] - G \quad (7)$$

where  $\omega$  is the swelling pressure,  $v_1$  is the molar volume of the solvent,  $\phi$  is the volume fraction of the polymer,  $R$  is the gas constant,  $T$  is the absolute temperature, and  $\chi_0$  and  $\chi_1$  are constants. The functional similarity of the osmotic isotherms suggests that in spite of substantial differences between these two polyelectrolytes their essential physicochemical properties are governed by the same interactions.

In the collapsed state (*i.e.* above the volume transition) osmotic measurements were not made. The dependence of the osmotic pressure on the polymer volume fraction in this region is schematized in the Figure (dashed curve). In the negative osmotic pressure region the gel expels solvent, and adjusts its volume so that the osmotic swelling pressure is zero.

The macroscopic physical properties of polymer systems are determined by the interplay of short- and long-range interactions that govern the organization of the molecules at different length scales. We used SANS to explore structural hierarchy of PAA and DNA gels as a function of the length scale in the spatial range of 1–100 nm.

In Figure 3, the SANS spectra of PAA and DNA gels are shown in the swollen state close to the volume transition. At low  $q$  ( $< 0.005 \text{ \AA}^{-1}$ )

power law behavior is observed of the form  $I(q) \propto q^{-m}$ , where  $m \approx 3.6$  (PPA) and 3.8 (DNA). This form of excess scattering, caused by surface scattering from large clusters ( $> 1000 \text{ \AA}$ ), is characteristic of polyelectrolyte solutions.<sup>18,27,28</sup> In the intermediate  $q$  range a linear region is distinguishable with a slope of  $-1$ . This behavior is typical of solutions containing linear (rod-like) structural elements.<sup>12</sup> As discussed in the theoretical section, in solutions of overlapping rod-like molecules the description of the thermodynamic concentration fluctuations requires two characteristic distance scales. The shoulder at high  $q$  ( $\approx 0.08 \text{ \AA}^{-1}$ ) can be associated with the second length, defined by the cross-sectional radius of the polymer chain ( $r_c$  in eq 2).

The continuous lines through the data points show the least squares fits to eq 5, and the dashed lines represent the thermodynamic component (first term in eq 5) of each fit. The thermodynamic component of the scattering intensity can be estimated independently from measurements of the osmotic swelling pressure,  $\omega$ , and the elastic (shear) modulus,  $G$ . In gels, because of their nonzero elasticity,  $K_{\text{os}}$  is replaced by the longitudinal osmotic modulus<sup>29</sup>

$$M_{\text{os}} = \phi \partial \omega / \partial \phi + 4/3 G \\ = \phi^2 (RT/v_1) [1/(1-\phi) - 2\chi_0 - 3\chi_1\phi] + G \quad (8)$$

In Figure 3, the arrows at the left axis show the scattering intensity in the thermodynamic limit  $I(q=0)$ , calculated from eq 8 and the known neutron scattering contrast of the respective polymer/

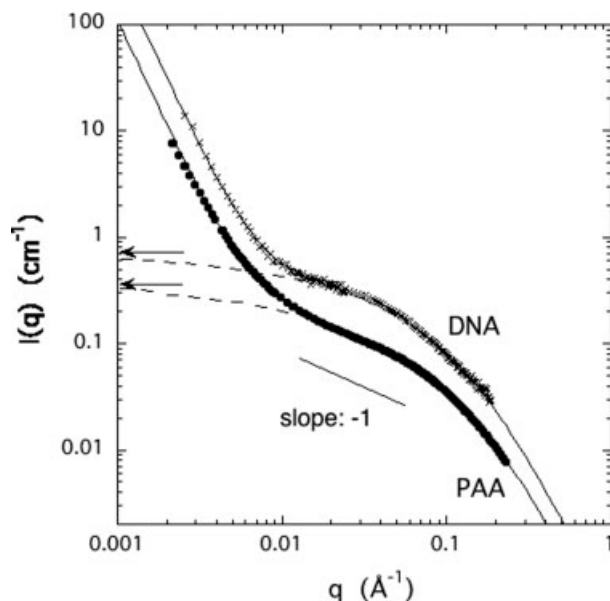


**Figure 3.** SANS spectra of PAA and DNA gels in 40 mM NaCl solution containing 0.8 mM  $\text{CaCl}_2$  (PAA) and 0.25 mM  $\text{CaCl}_2$  (DNA). Continuous lines are the fits to eq 5. Dashed lines are the osmotic components of the fits. Arrows indicate the scattering intensity estimated from macroscopic swelling pressure and shear modulus measurements.

solvent system. The intensities thus obtained from macroscopic observations are in reasonable agreement with the SANS results.

In Figure 4, the SANS spectrum of a HA gel is compared with that of the corresponding (uncrosslinked) HA solution. The scattering intensity from the gel slightly exceeds that of the solution. At low  $q$  the difference is small, indicating that crosslinking does not modify significantly the large clusters that are present in the solution before introducing the crosslinks. At the high- $q$  side the downturn occurs nearly at the same  $q$ . In this region the scattering response is governed by the structure factor of the polymer chain. In the intermediate  $q$ -range the increase in scattering intensity reflects the effect of crosslinks on the organization of the polymer strands. Gel formation is generally accompanied by redistribution of the polymer molecules: in the vicinity of the crosslinks the local polymer concentration increases, while between the polymer-rich regions the concentration diminishes. Previous studies on various polymer gels suggest that the latter “solution-like” matrix governs the thermodynamic properties of the gel.<sup>30–32</sup> The SANS spectra of both HA gel and solution can be satisfactorily described by eq 5 (continuous lines in Fig. 4). Note that the osmotic modulus

of the lightly crosslinked HA gel ( $M_{os} = 24$  kPa) differs only slightly from that of the corresponding HA solution ( $K_{os} = 26$  kPa).

In Figure 5 are shown the SANS spectra of DNA and PASP solutions. These polymers display a similar scattering response to the HA solution. For small values of  $q$  ( $< 0.01 \text{ \AA}^{-1}$ ) the decrease of the intensity can be fairly well described by a simple power-law with a slope of  $-3.6$  (PASP) and  $-3.9$  (DNA). This behavior can be attributed to surface scattering of clusters of size greater than several thousand ångströms. It is remarkable that such large objects exist in solutions of charged polymers. Clusters can be stable only if there is an overall attraction. In DNA solutions, for example, clusters consisting of closely packed phosphate residues possess an enormous negative charge. Although the underlying mechanism of cluster formation is poorly understood, some suggestions have been put forward in the literature. Schmitz introduced the concept of “temporal aggregates” and attributed the attractive interactions to fluctuating dipolar interactions because of an asymmetric distribution of counterions around the polyelectrolyte chain.<sup>27</sup> Attractive interactions of nonelectrostatic origin may also play a role in solutions of highly charged polyelectrolytes.<sup>28,33</sup> In the present solutions, the power law dependence is followed by a linear region ( $0.02 \text{ \AA}^{-1} < q < 0.1 \text{ \AA}^{-1}$ ) and a shoulder at high  $q$  ( $\approx 0.1 \text{ \AA}^{-1}$ ). The values obtained

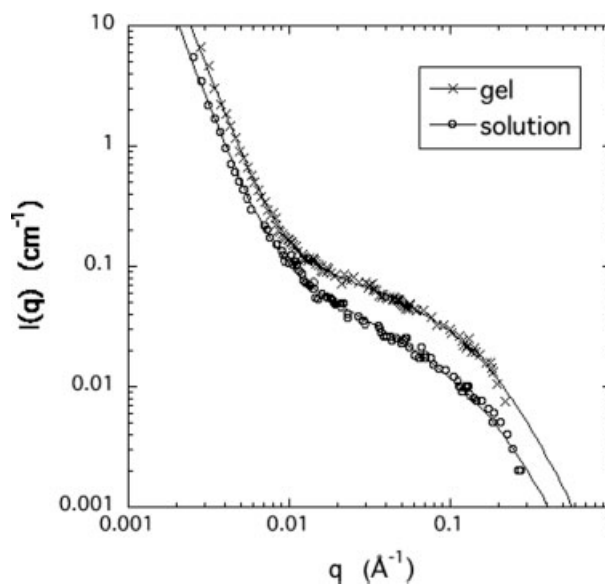


**Figure 4.** SANS spectra of a 3% (w/w) HA gel and the corresponding uncrosslinked solution. The measurements were made in 100 mM NaCl solution. Continuous curves show the least squares fits of eq 5 to the data.

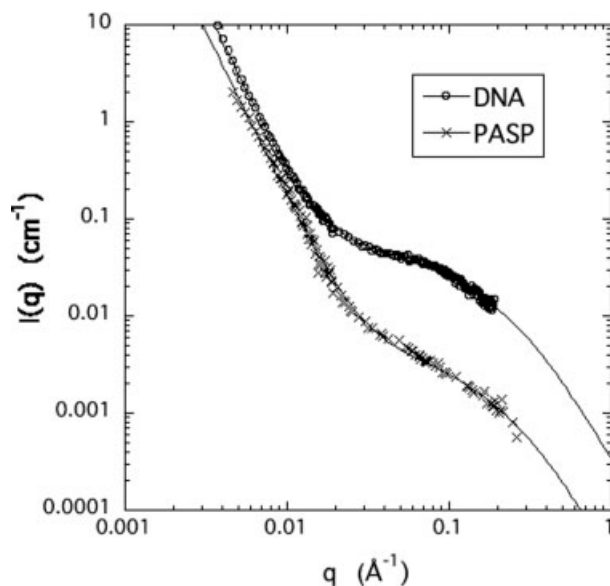


**Figure 5.** SANS spectra of DNA and PASP solutions. The measurements were made in 100 mM NaCl solution. The polymer concentration is 3% (w/w). The continuous lines show the least squares fits of eq 5 to the data.

for  $L$  and  $r_c$  from the fits of eq 5 to the SANS measurements in HA, DNA, and PASP solutions are listed in Table 1.

In spite of major differences in the chemical architecture and physical properties of these biopolymers, (e.g., type of chemical backbone, monomer size and structure, chain rigidity) there are no marked differences in their SANS response. DNA consists of two polynucleotide chains that are twisted into a double-stranded helix. The two DNA strands are kept together through hydrogen bonds between the bases. The persistence length of the DNA chain is about 50 nm.<sup>34</sup> In the HA molecule disaccharide units, consisting of D-glucuronic acid and D-N-acetylglucosamine, are connected through alternating  $\beta$ -1,4 and  $\beta$ -1,3 glycosidic bonds. In solution, high molecular weight HA chains form an entangled network through steric interactions and self-association between the individual molecules.

**Table 1.** Fitting Parameters of eq 5 to the SANS Spectra of Biopolymer Systems (3% w/w)

Polymer System	$L$ (Å)	$r_c$ (Å)
DNA solution	$8 \pm 3$	$9.6 \pm 2$
HA gel	$22 \pm 5$	$4.7 \pm 1$
HA solution	$26 \pm 6$	$5.1 \pm 1$
PASP solution	$18 \pm 4$	$3.5 \pm 1$

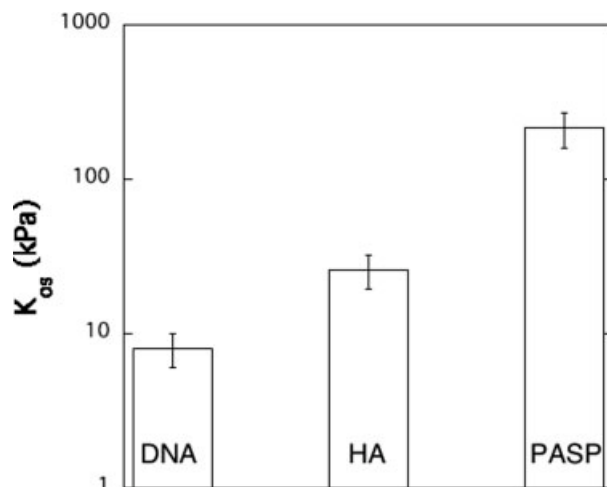


**Figure 6.** Osmotic compression modulus,  $K_{os}$ , of biopolymer solutions. The values of  $K_{os}$  were determined from the analysis of the SANS spectra (see text).

The persistence length of the HA molecule is about 20 nm.<sup>35</sup> Poly(aspartic acid) is a synthetic polypeptide in which the amino acid units joined together by peptide bonds carry a carboxyl group. Interactions between these negatively charged molecules are repulsive, and in physiological salt solutions PASP chains assume a random coil configuration. The persistence length of PASP is about 2 nm.<sup>36</sup>

Finally we compare the osmotic modulus,  $K_{os} = \varphi(\partial\Pi/\partial\varphi)$ , of the three different biopolymer solutions.  $K_{os}$  controls the amplitude of the osmotic concentration fluctuations in the thermodynamic limit, that is at  $q \rightarrow 0$ .  $K_{os}$  is inversely proportional to the scattering intensity (see for example eq 2) and can be determined from the SANS spectrum. Figure 6 shows the values of  $K_{os}$  for the three types of representative biopolymers having identical polymer concentrations.  $K_{os}$  increases in the order DNA < HA < PASP, which is opposite to the trend in the variation of the persistence length. We interpret this finding in terms of the general tendency for strongly interacting rigid chain segments to organize into correlated domains or even bundles, which in turn causes a drop in the osmotic pressure and the osmotic modulus. It is known that stiff polymer chains in solutions can undergo a sharp collapse from a spatially extended conformation to a compact one.<sup>37</sup> For example, enhanced rigidity of double-stranded DNA compared to the single strand leads to sharp, controllable conformational transitions. Of course, other factors besides chain rigidity (e.g., electrostatic interactions, charge density, ion binding, solvent quality) also contribute to the osmotic modulus, and these

must be considered for a more complete understanding of the variation of the osmotic modulus.

## CONCLUSIONS

In this paper we made three comparisons. (1) It is found that synthetic (PAA) and biopolymer (DNA) gels exhibit similar osmotic and scattering properties. The SANS results suggest that the interactions between polyelectrolyte chains and the surrounding small ions govern the equilibrium structure and the osmotic concentration fluctuations in these systems. (2) Comparison of the scattering response of crosslinked and uncrosslinked polymers indicates that crosslinking slightly increases the scattering intensity. However, the overall shape of the SANS spectrum remains unchanged. (3) The SANS results show that the structure of entirely different biopolymer solutions (DNA, HA, PASP) is affected only weakly by the fine details of the architecture of the polymer chains (size and chemical structure of the monomer unit, type of polymer backbone, *etc.*).

For the solutions of these three representative biopolymers, the osmotic compression modulus determined from the analysis of the SANS spectra decreases with increasing persistence length of the chain.

This research was supported by the Intramural Research Program of the NIH, NICHD. The authors acknowledge the support of the National Institute of Standards and Technology, U.S. Department of Commerce for providing access to the NG3 small angle neutron scattering instrument used in this experiment. This work is partially based upon activities supported by the National Science Foundation under Agreement No. DMR-9423101.

## REFERENCES AND NOTES

- Katchalsky, A.; Lifson, S.; Eisenberg, H. *J Polym Sci* 1951, 7, 571–574.
- Katchalsky, A.; Michaeli, I. *J Polym Sci* 1955, 15, 69–86.
- Tanaka, T. *Phys Rev Lett* 1978, 40, 820–823.
- Tanaka, T.; Fillmore, D. *J Chem Phys* 1979, 70, 1214–1218.
- Ricka, J.; Tanaka, T. *Macromolecules* 1984, 17, 2916–2921.
- Tasaki, I. *Jpn J Physiol* 1999, 49, 125–138.
- Tasaki, I.; Byrne, P. M. *Biopolymers* 1994, 34, 209–215.
- Widom, J.; Baldwin, R. L. *J Mol Biol* 1980, 144, 431–453.
- Eickbush, T. H.; Moudrianakis, E. N. *Cell* 1976, 13, 295–306.
- Douzou, P. *Proc Natl Acad Sci USA* 1987, 84, 6741–6744.
- de Gennes, P. G. *Scaling Concepts in Polymer Physics*; Cornell University Press: Ithaca, NY, 1979.
- Higgins, J. S.; Benoit, H. C. *Polymers and Neutron Scattering*; Clarendon Press: Oxford, 1994.
- Horkay, F.; Grillo, I.; Basser, P. J.; Hecht, A. M.; Geissler, E. *J Chem Phys* 2002, 117, 9103–9106.
- Horkay, F.; Hecht, A. M.; Mallam, S.; Geissler, E.; Rennie, A. R. *Macromolecules* 1991, 24, 2896–2902.
- Geissler, E.; Horkay, F.; Hecht, A. M. *Phys Rev Lett* 1993, 71, 645–648.
- Horkay, F.; Basser, P. J.; Hecht, A. M.; Geissler, E. *Polymer* 2005, 46, 4242–4247.
- Williams, C. E.; Nierlich, M.; Cotton, J. P.; Jannink, G.; Boue, F.; Daoud, M.; Farnoux, B.; Picot, C.; de Gennes, P. G.; Rinaudo, M.; Moan, M.; Wolf, C. J. *J Polym Sci Lett Ed* 1979, 17, 379–384.
- Zhang, Y.; Douglas, J. F.; Ermi, B.; Amis, E. *J Chem Phys* 2001, 114, 3299–3313.
- Horkay, F.; Tasaki, I.; Basser, P. J. *Biomacromolecules* 2000, 1, 84–90.
- Horkay, F.; Basser, P. J. *Biomacromolecules* 2004, 5, 232–237.
- Horkay, F.; Tasaki, I.; Basser, P. J. *Biomacromolecules* 2001, 2, 195–199.
- NIST Cold Neutron Research Facility, NG3 and NG7 30-m. SANS Instruments Data Acquisition Manual, 1999.
- Horkay, F.; Zrinyi, M. *Macromolecules* 1982, 15, 1306–1310.
- Vink, H. *Eur Polym J* 1971, 7, 1411–1419.
- Treloar, L. R. G. *The Physics of Rubber Elasticity*; Clarendon Press: Oxford, 1976.
- Flory, P. J. *Principles of Polymer Chemistry*; Cornell University Press: Ithaca, NY, 1953.
- Schmitz, K. S.; Lu, M.; Gaunnt, J. *J Chem Phys* 1983, 78, 5059–5066.
- Tanahatoo, J. J.; Kuil, M. E. *J Phys Chem B* 1997, 101, 9233–9239.
- Landau, L. D.; Lifshitz, E. M. *Theory of Elasticity*; Pergamon Press: London, 1986.
- Horkay, F.; Hecht, A. M.; Geissler, E. *J Chem Phys* 1989, 91, 2706–2711.
- Horkay, F.; Burchard, W.; Geissler, E.; Hecht, A. M. *Macromolecules* 1993, 26, 1296–1303.
- Horkay, F.; Burchard, W.; Hecht, A. M.; Geissler, E. *Macromolecules* 1993, 26, 3375–3380.
- Wissenburg, P.; Odijk, T.; Cirkel, P.; Mandel, M. *Macromolecules* 1995, 28, 2315–2328.
- Bloomfield, V. A. *Biopolymers* 1977, 44, 269–282.
- Cleland, R. L. *Arch Biochem Biophys* 1977, 180, 57–68.
- Raman Research Institute, Annu Report 2001–2002, Bangalore.
- Diamant, H.; Andelman, D. *Phys Rev E: Stat Phys Plasmas Fluids Relat Interdiscip Top, Part B* 2000, 61, 6740–6749.